CHAPTER 6. Mechanical Performance Studies.

1. Introduction.

In order to restrict the change in magnetic field harmonics over the operational field range and reduce the probability of spontaneous quenches caused by conductor motion, the coil turns must be mechanically constrained. This constraint is achieved by applying stress to the coil during magnet fabrication, compressing it into an essentially rigid cavity, which supports it during operation. This azimuthal mechanical support and prestress of the HGQ coil is completely provided by the stainless collars. Thick steel end plates are used to restrict the longitudinal coil motion under Lorentz forces. The required prestress that is to be applied to the magnet coils at room temperature which will compensate the prestress decrease resulting from collar spring back, coil creep, difference in the coil and collar thermal contraction and Lorentz forces during magnet excitation, is chosen based on results of finite element analysis [1].

In order to verify experimentally that the chosen design and prestress range would satisfy the mechanical requirements, a complementary program of FEM analysis and short model tests was employed. The primary areas of concern were:

- conductor mechanical stability and coil azimuthal prestress
- longitudinal coil contraction and support against Lorentz forces

Coil size and E-modulus optimization is itself a significant effort with pronounced bearing on magnet mechanical and magnetic performance, and is described in Chapter 2. The results of mechanical measurements performed on HGQ short models at room and helium temperatures are summarized in this Chapter.

2. Instrumentation.

After fabrication and room temperature tests are completed, the model magnets undergo thorough cryogenic testing in the Fermilab Vertical Magnet Test Facility (VMTF) [2]. Instrumentation used for the mechanical studies includes:

- strain gauges (resistive and capacitative) installed in the magnet straight section in order to measure azimuthal stress
- bullet gauges/load screws installed in the end plates to provide and monitor longitudinal force
- shell gauges to measure strain in the cold mass shell

In addition to direct measurements of mechanical parameters, field harmonics measurements taken over the operational cycle were also used to investigate and quantify azimuthal and radial coil motion under the influence of Lorentz forces.

The beam and capacitance gauges for measuring coil azimuthal stresses have been specifically designed for the HGQ magnet cold masses. These gauges utilize technology identical to that employed in previous superconducting magnet development projects [3, 4]. Likewise, the bullet gauges used for measuring longitudinal coil forces are identical in nature to those used, for example, in the SSC magnet development program, with suitable modifications for the present cold mass [5]. As a result, the level of information provided by this instrumentation is comparable to that of previous magnet development efforts.

Beam and capacitance gauges are installed in the straight section of the collared coil assembly. Typically one pair of gauges will record the inner coil stress, while another records the outer coils stress. They are arranged so that two beam gauges are in diametrically opposed quadrants, while two capacitance gauges are placed in the remaining two quadrants, in the same coil cavity as a corresponding beam gauge. The gauges are typically installed near the middle of the magnet, where coil size is smallest (and hence, coil stress lowest). Initially some cold masses had two gauge packs installed, with the second one near the non-lead end, but as the coil sizes were typically larger there (and coil stress measurements less likely to be of interest), and the installation of instrumentation always incorporates some non-zero risk of adverse performance effects, use of the second instrumented gauge pack was discontinued.

Commercially available strain gauges [6] were also mounted directly to the cold mass shell, in order to measure strains arising from Lorentz forces during magnet excitation. Initially, gauges were mounted to measure longitudinal strains at both ends of the magnet. As no asymmetry was noted, subsequent installations were restricted to measuring strains over the return-end half of the cold mass shell only. On a few cold masses, azimuthal strains were measured, but since this is of little interest to magnet mechanics (simply representing the Poisson effect of a longitudinally strained cylinder), the latest shell gauge applications have been exclusively longitudinal. The shells on the latest cold masses were instrumented with two sets of longitudinally oriented gauges, measuring strains along the quadrant 1 axis, and at 45 degrees from it, as shown in the Figure 1 below.

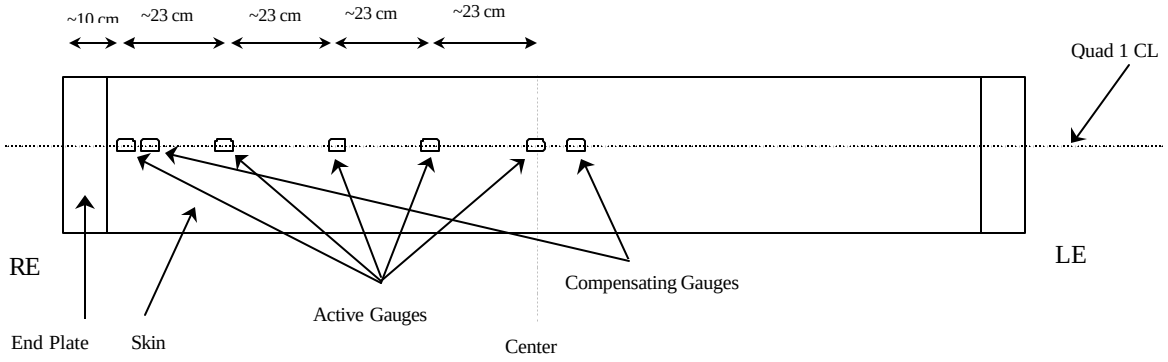

Figure 1. Position and orientation of shell gauges on the cold mass skin as used in magnets HGQ07-09

With the exception of the shell gauges, which only measured relative strains, all of the gauges used to measure azimuthal and longitudinal coil stress were calibrated at both 300K and 4.3 K. Gauges were "trained" 5 times to 125% of their working limits to

eliminate zero-strain shifts, and then three calibration runs were performed in succession to ensure reproducible results. Strain-free offsets for the resistive gauges were also measured at 1.9 K. Very good calibration reproducibility resulted, typically better than 1.4 MPa for beam and capacitance gauges, and 0.4 kN for bullet gauges [7, 8]. Measurement reproducibility during cryogenic magnet testing (between thermal cycles) was typically on the order of a few percent.

During cold mass fabrication, coil stress is measured during the collaring process, and before and after the shell is welded. After the end plates are attached, coil longitudinal force is monitored while the ends are pre-loaded. During cryogenic testing, coil stresses, skin stresses, and longitudinal coil forces are measured for each excitation cycle, as a function of applied current. Coil stresses and longitudinal end forces are also recorded at cryogenic temperatures before excitation, to provide information on stress and force changes due to thermal contraction effects upon cooldown from room temperature.

3. Test results.

A. Azimuthal stress measurements.

Along with measurements taken during fabrication, coil stress is routinely measured during quench testing. Typical inner and outer coil stress measurement results during quench testing of magnets HGQ01 and HGQ02 are given in Figure 2. The linear decrease in coil stress is in excellent agreement with that expected from the I^2 dependence of the Lorentz forces exerted on the conductor. Both magnets HGQ01 and HGQ02 exhibited satisfactory azimuthal coil stress at the maximum current reached during testing, and would indeed maintain non-zero coil stress at the nominal field gradient.

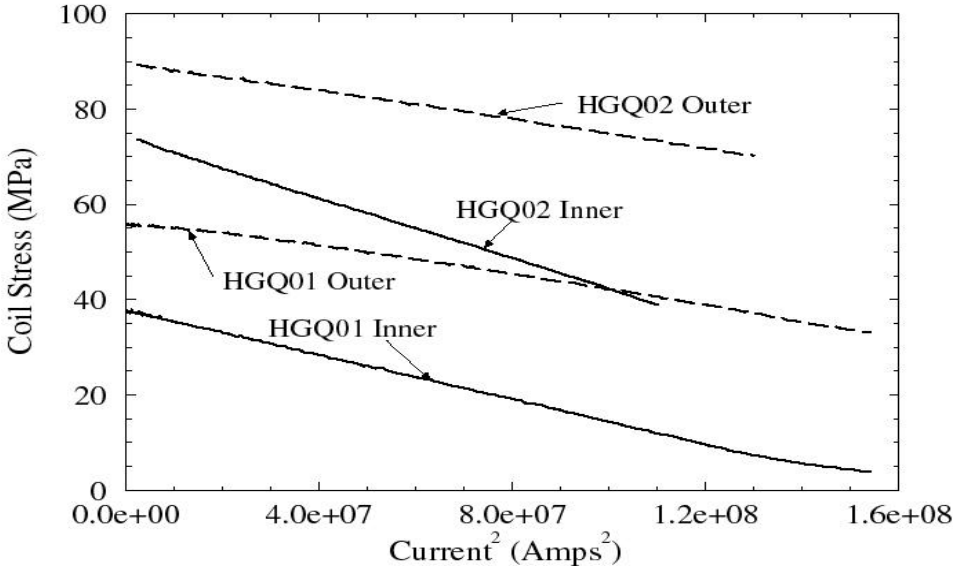

Figure 2. Average azimuthal stress for the inner and outer coils of magnets HGQ01 and HGQ02, as a function of excitation current.

A typical example of outer coil azimuthal stress as a function of excitation current for magnets HGQ05 and 07 is given in Figure 3. Due to yielding effects with inner coil strain gauges in earlier HGQ magnets, they were omitted from this latest series [7]. In this figure we once more see the essentially linear decrease of coil stress with $(I_{mag})^2$, in excellent agreement with expectations.

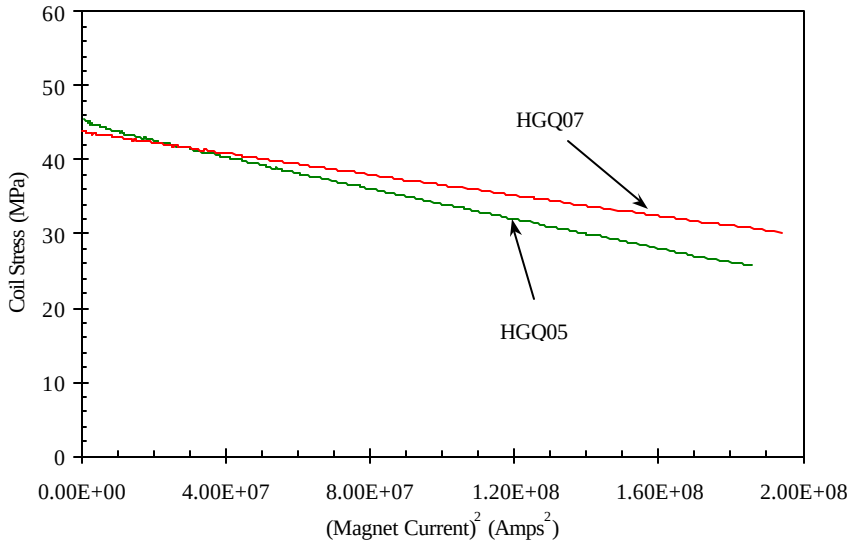

Figure 3. Average outer coil azimuthal stress for magnets HGQ05,07 at 1.9K.

The inner and outer coil azimuthal stress for a later magnet, HGQ09, is shown in Figure 4. Again the linear dependence of coil stress with the square of the excitation current is readily observed. Further, no unloading of the coils is evident even at the highest currents reached, indicating positive contact between the coils and constraining structure is maintained throughout the operational range.

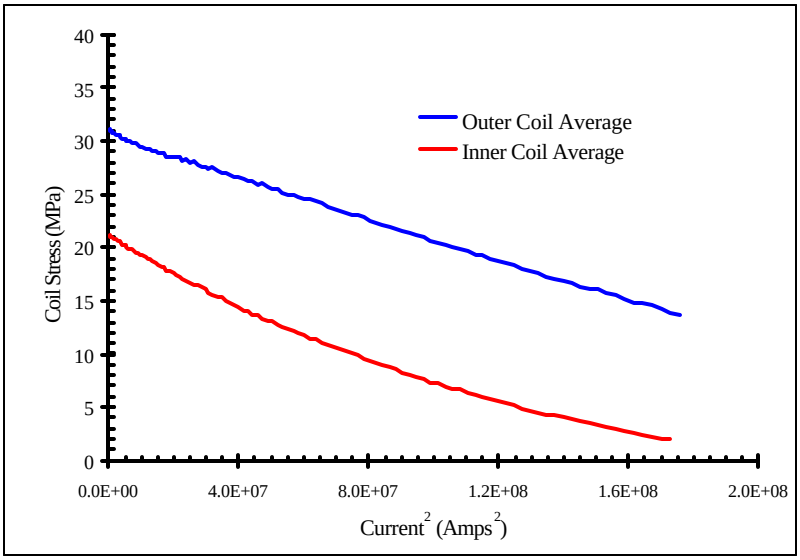

Figure 4. Inner and outer coil azimuthal stress for magnet HGQ09, as a function of excitation current.

Results from coil stress measurements performed at room temperature and under cryogenic operating conditions for the series of short model magnets are summarized in Table 1. The data suggest that no unloading of the coil was observed up to the highest operating currents reached during testing. Coil deformation due to Lorentz forces appeared to be elastic over this range.

Table 1. Azimuthal Coil Stress and Lorentz Force.

Model Number	Azimuthal prestress 300K		Azimuthal prestress 1.9K		Azimuthal Lorentz force	
	Inner layer, MPa	Outer layer, MPa	Inner layer, MPa	Outer layer, MPa	Inner layer, MPa/kA^2	Outer layer, MPa/kA^2
Design	81	81	74	66	-0.28	-0.20
HGQ01	67	72	38	58	-0.28	-0.13
HGQ02	73	94	76	84	-0.31	-0.15
HGQ03	187	97	173	102	-0.29	-0.13
HGQ05	99	55	-	49	-0.24C	-0.13
HGQ06	59C	61C/139B	-	169B	-0.41C	-0.26B/-0.08C
HGQ07	65C	74C/58B	-	45B	-0.16C	-0.11B/-0.06C
HGQ08	86C/94B	92C/96B	66B	105B	-0.20C/-0.28B	-0.16B/-0.06C
HGQ09	68C/48B	77C/58B	33B	42B	-0.26C/-0.16B	-0.11B/-0.10C

(Note : "B" indicates beam gauge data, "C" indicates capacitance gauge data)

Over the course of building the series of short model magnets, the azimuthal prestress of the coils was changed from ~ 60-100 MPa in the inner layer and ~ 55-100 MPa in the outer layer, to study the effects of prestress (and prestresss distribution) on magnet performance. The exceptional values of inner coil prestress in magnet HGQ03 and outer coil prestress in magnet HGQ06 at room temperature are believed to be due to instrumentation errors. Following magnet HGQ05, the coil/shim sizes were adjusted so that the inner and outer coil prestresses were more evenly matched, and the range of prestress employed was narrowed.

Prestress changes upon cooldown from 300K to 1.9K were typically ~ 15-25 MPa in the inner coil and 10-15 MPa in the in outer coil, based on analysis of the most reliable data. The inner coils showed somewhat larger cooldown losses than anticipated by FEA calculations while the outer coils matched the calculation more closely. The increased cooldown loss observed in the inner coil did not, however, lead to any condition where the inner coils were observed to unload during operation.

Coil stress change under the influence of Lorentz forces agrees reasonably well with model predictions. The stress reduction in the outer coils is somewhat lower than anticipated, most likely due to frictional effects at the inner/outer coil and outer coil/collar boundaries, which inhibit outer coil motion somewhat. This effect is also seen in the model magnet which had the lowest initial prestress (HGQ06). As the interface friction is proportional to the level of prestress in the coils, this magnet showed a larger response to Lorentz forces, due to the presumably lower friction.

B. Harmonics changes during current ramp cycle

Significant conductor motion during current ramping can lead to changes in the value of certain allowed harmonics (b_6, b_{10}) as a function of current (neglecting iron saturation

effects). This has not been observed in any of the HGQ model magnets, as evidenced by Figure 5, which shows the dodecapole as a function of current during a ramp for magnet HGQ09. Only data for currents > 5000 A are shown, to eliminate the effects of SC and iron magnetization hysteresis. Note that there is no appreciable change over the (up/down averaged) ramp cycle, indicating that conductor motions large enough to affect the magnetic field quality are not present.

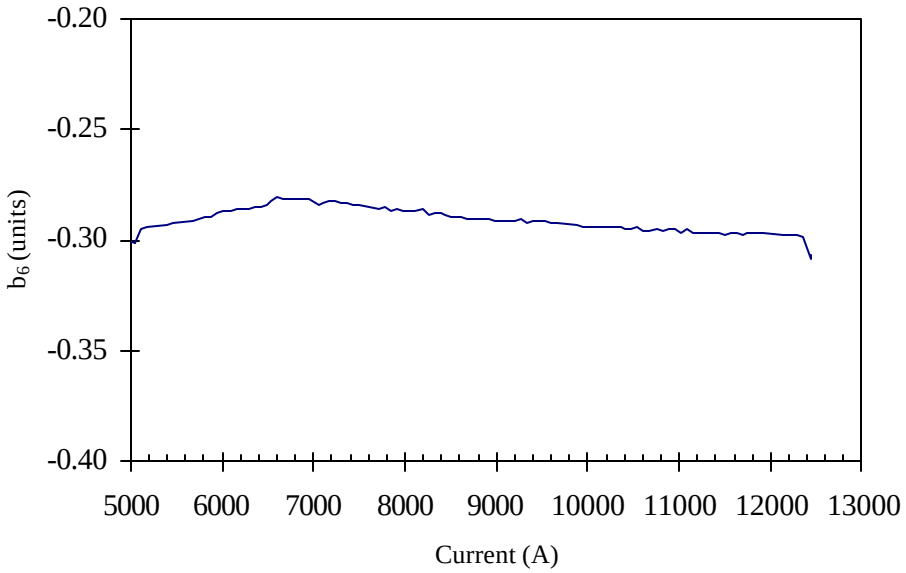

Figure 5. Average value (up/down ramp) of b_6 during a current ramp cycle for magnet HGQ09.

C. Longitudinal coil performance

Longitudinal coil force is initially measured when the end loading bolts are tightened during final assembly of the cold mass. This is done to ensure that adequate contact between the coil and end (restraint) plates is maintained upon cooldown. The required level of preloading has been determined by empirical studies under cryogenic conditions.

During model magnet testing, the longitudinal coil force is measured upon cooldown from 300K to1.9K, and during excitation (quench testing). The longitudinal end force measurement for magnet HGQ01 during cryogenic testing is shown in Figure 6. The lower set of curves are measurements taken during the first test cycle. No end force is observed at the non-lead end for currents below about 7000A, indicating that the coils had shrunk upon cooldown more than the yoke/shell, leading to a loss of contact with the end plates. Since the majority of quenches observed in magnet HGQ01 were located in the transition area between the coil ends and straight section, it was decided to increase the longitudinal coil pre-load between cryogenic test cycles, in order to determine if improved longitudinal restraint would have a beneficial effect on quench performance. This was done, and is evident from the upper set of curves in Figure 6, which show that now both ends are supported at all levels of excitation current. This improved longitudinal restraint did not have an observable effect on quench behavior - magnet

HGQ01 still trained substantially, and the majority of quenches during the second test cycle were still localized in the magnet ends and transition area.

Concerns with very high end-loads at elevated excitation current levels leading to mechanical failure of the coil end part material led to the decision to apply an intermediate longitudinal pre load to magnet HGQ02. Cryogenic testing, however, showed that the chosen room-temperature pre-load was insufficient to maintain end plate-coil contact in all quadrants of the magnet when at liquid Helium temperatures. As shown in Figure 7, only one quadrant of the magnet was in contact with the end restraining plate at zero excitation current. Magnet HGQ02 experienced a majority of training quenches in the coil non-lead end regions, corresponding to the least loaded end of the magnet. The end region quenches of magnet HGQ02 occurred farther into the end region of the coils, not in the transition region. This may have been due to poor end part/coil adhesion resulting from a change in end part material and coil insulation adhesive properties, a problem corrected on HGQ03. During quench training, it was observed that coil-end plate contact was initially occurring at subsequently lower excitation currents, indicating that the longitudinal coil motion was not reversible. During its second test cycle the end pre-load was completely removed from the non-lead end (the lead end loading screws are inaccessible once the quadrant splices are completed). Upon the resumption of cryogenic testing, no appreciable change in quench performance was observed. It would appear that longitudinal end force alone is not sufficient in this case to mechanically stabilize the end regions of the coils.

The total end forces measured for magnets HGQ01and HGQ02 are significantly lower than expected. The additional end loads resulting from Lorentz forces acting on the coil during excitation are about a factor of four smaller than calculated, based upon the assumption that the total longitudinal force on the coils is transferred to the end restraint plates. It would appear, therefore, that either some longitudinal load was being transferred radially to the yoke and skin, or the cable turns in the end regions of the coils were perhaps separating, leaving only a small fraction of the turns to transfer the longitudinal load to the end plates.

In subsequent magnets, radial support and azimuthal compression of the coil ends is provided by an aluminum end can and G-11 collets. The profiles of the end can and collets are tapered so that as they are installed longitudinally, they provide radial compression and support. Longitudinal support of the coils is provided by stainless steel end plates that are welded to the outer shell. Loading screws (bullets) mounted into the end plates apply longitudinal load to the coils. In magnets HGQ06 and later, the end cans are bolted to the end plates ostensibly to minimize coil displacement away from the end plates during cooldown. Longitudinal expansion towards the end plates during excitation is reacted only by the bullets.

The longitudinal coil force as a function of excitation current for magnets HGQ05 and HGQ06 is given in Figure 8, which shows that positive contact between the ends of the coils and the loading screws was maintained upon cooldown, ensuring adequate support of the coils during excitation. In previous model magnets end restraint was not always maintained after cooldown due to thermal contraction of the coils, or was maintained by requiring excessive longitudinal preload at 300K. Use of the aluminum end cans and G-10/G-11 end part materials has alleviated this problem in the latest series of models, beginning with magnet HGQ05. The end load resulting from Lorentz forces

acting on the coil during excitation are still about 25% of the calculated Lorentz force, however. Figure 9 shows the end load of magnet HGQ08, which exhibits behavior similar to magnets HGQ05-07.

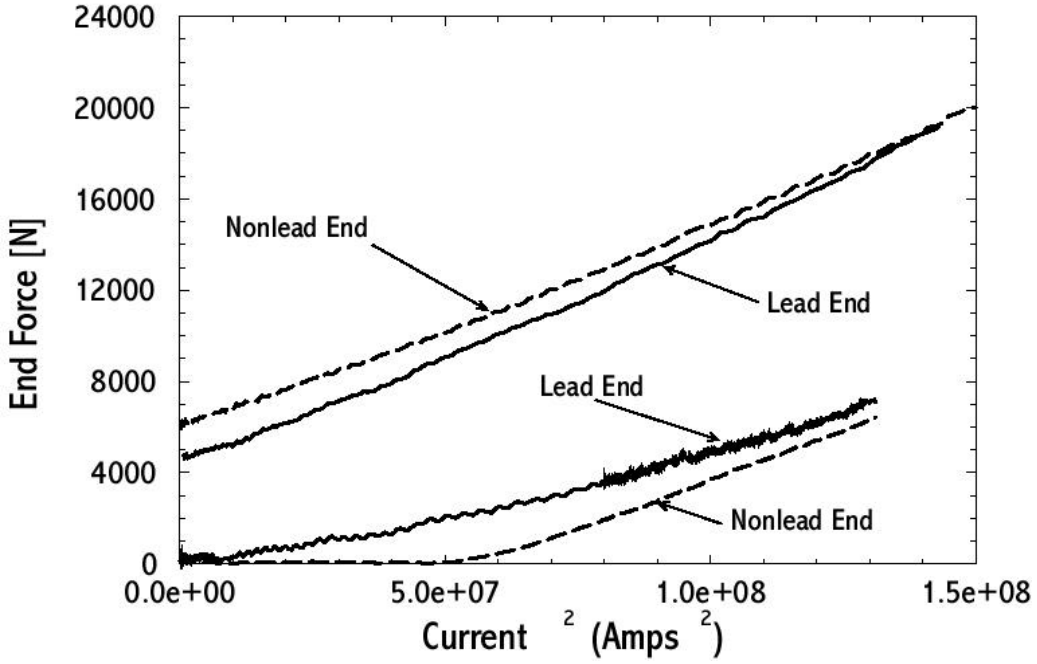

Figure 6. Total end force on magnet HGQ01 during the first and second test cycles. The non-lead end force was increased between test cycles. The lower set of curves are from the first test cycle, the upper set from the second.

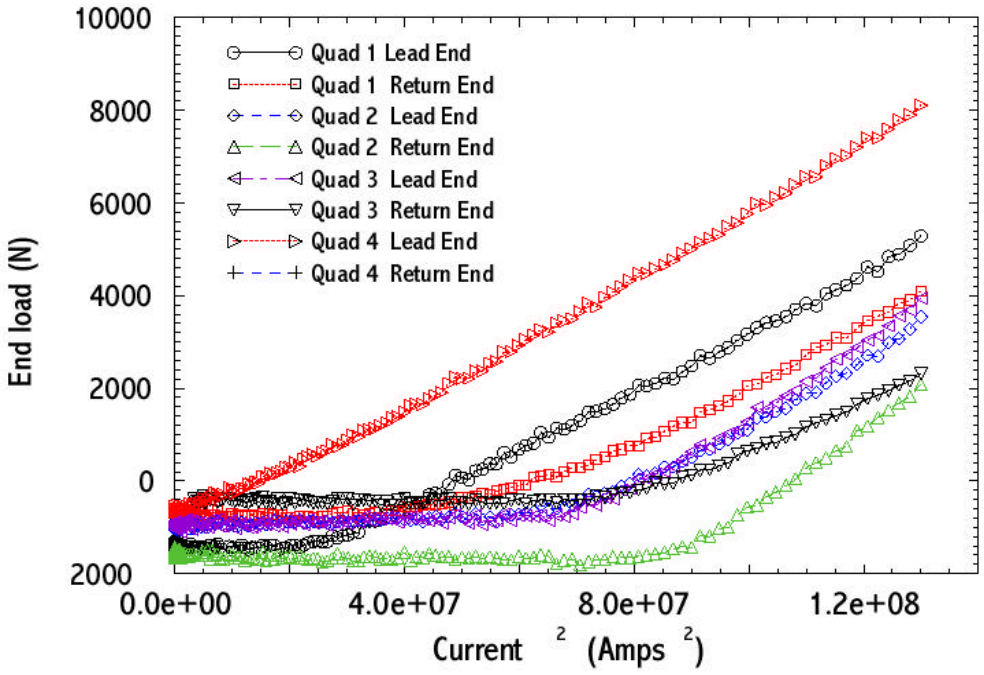

Figure 7. Individual quadrant end force on magnet HGQ02 as a function of excitation current during the first cryogenic test cycle.

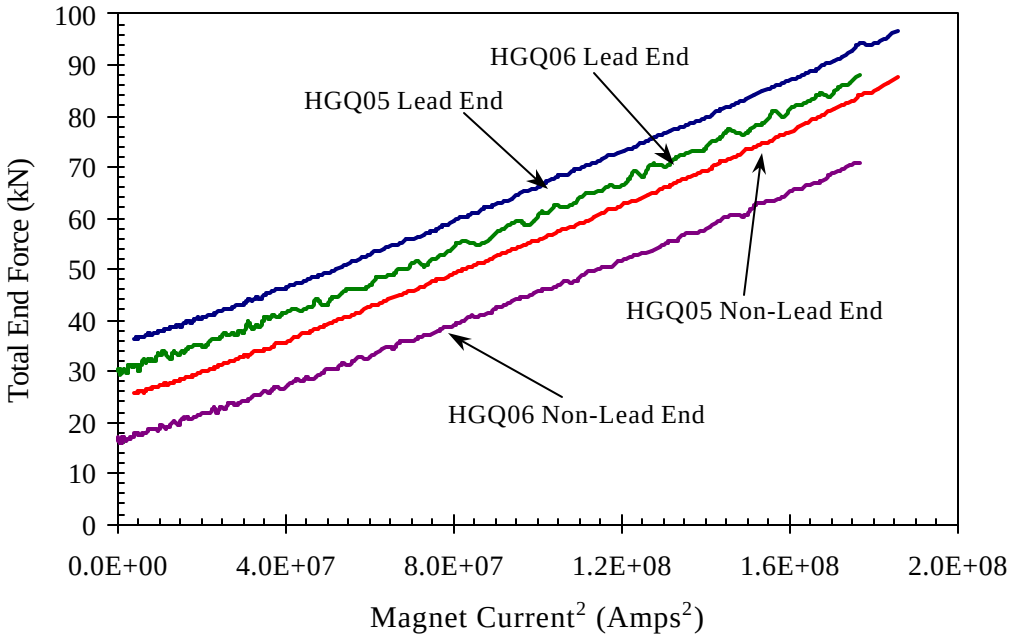

Figure 8. Total coil end loads for magnets HGQ05 & HGQ06 at 1.9K.

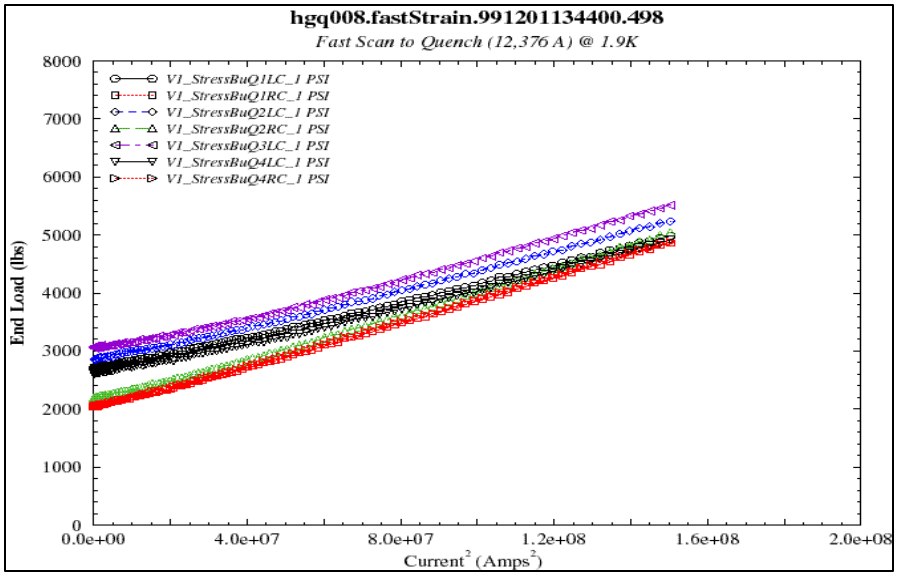

Figure 9. Coil end loads at 1.9K for magnet HGQ08

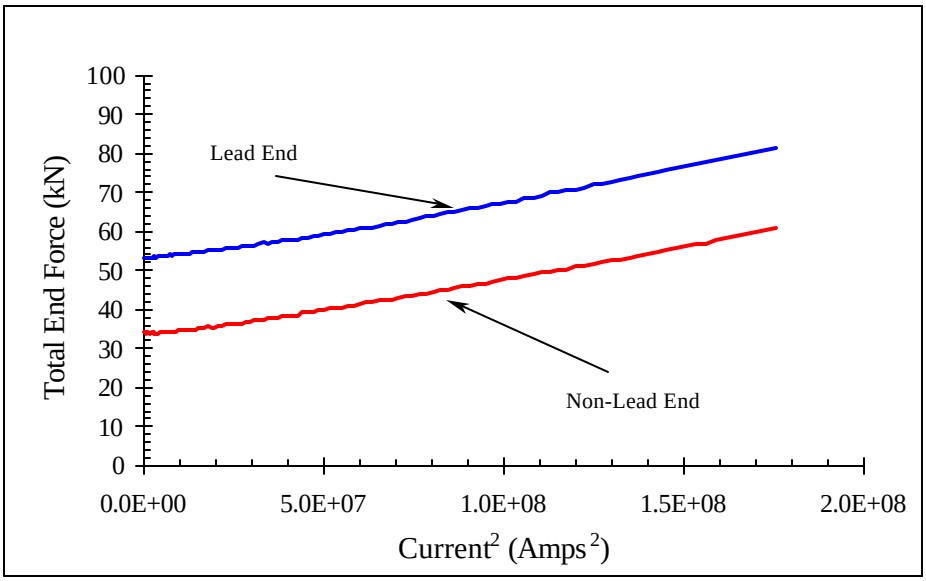

Figure 10. Total coil end loads for magnets HGQ09 at 1.9K.

The room temperature, cryogenic, and dynamic end force behavior of the HGQ model magnets is summarized in Table 2. Before employing the end can/collet system to provide radial and longitudinal restraint of the coils, the preload loss upon cooldown was greater than 13-14 kN. Beginning with magnet HGQ05, the cooldown loss was reduced to about 5 kN, and was observed to be further reduced to about 1 kN in magnets HGQ07-09. The primary reduction in cooldown loss can be ascribed to the additional support of the end can system, which greatly prevents the coils from shrinking from the end plates.

Table 2. Longitudinal Force and Lorentz Force per Quadrant.

Model number	Longitudinal end prestress 300K		Longitudinal end prestress 1.9K		Longitudinal Lorentz force	
	Lead end, kN	Return end, kN	Lead end, kN	Return end, kN	Lead end, kN/kA^2	Return end, kN/kA^2
Design	>0	>0	>0	>0	0.36	0.36
HGQ01	0.8/14.3	0.8/22.4	0/0.9	0/3.2	0.09	0.09
HGQ02	7.5	11.4	0	0	0.08	0.07
HGQ03A	8.2	8.3	0	0	0.06	0.06
HGQ05	10.5	10.2	5.1	4.1	0.089	0.091
HGQ06	9.4	9.4	4.7/6.2	3.0/3.0	0.088	0.083
HGQ07	11*	8*	10.5	7.5*	0.085	0.094
HGQ08	8.4/8.5	9.0/9.3	10.7/11.3	8.0/9.0	0.077/0.082	0.089/0.089
HGQ09	11	9	11.5	7.5	0.046	0.043

(* for 3rd test cycle where non-zero preload applied)

D. Skin stress measurement

Relative longitudinal strain is also measured as a function of length along the cold mass during excitation. In general, the measured strains at the magnet ends match that

expected from the measured coil end forces transferred to the end plate. The longitudinal strain sensitivity along the cold mass is shown in Figure 11 for magnets HGQ05-07. Magnet HGQ07 and later models were only instrumented along half of their length (from non-lead end to center), but in two different azimuthal positions (0 and 45 degrees with respect to the quadrant 1 axis). Since the non-lead end loading screws were not tightened for magnet HGQ07, no load was applied to the non-lead end plate. This is confirmed by the zero strain sensitivity measured at the end plates.

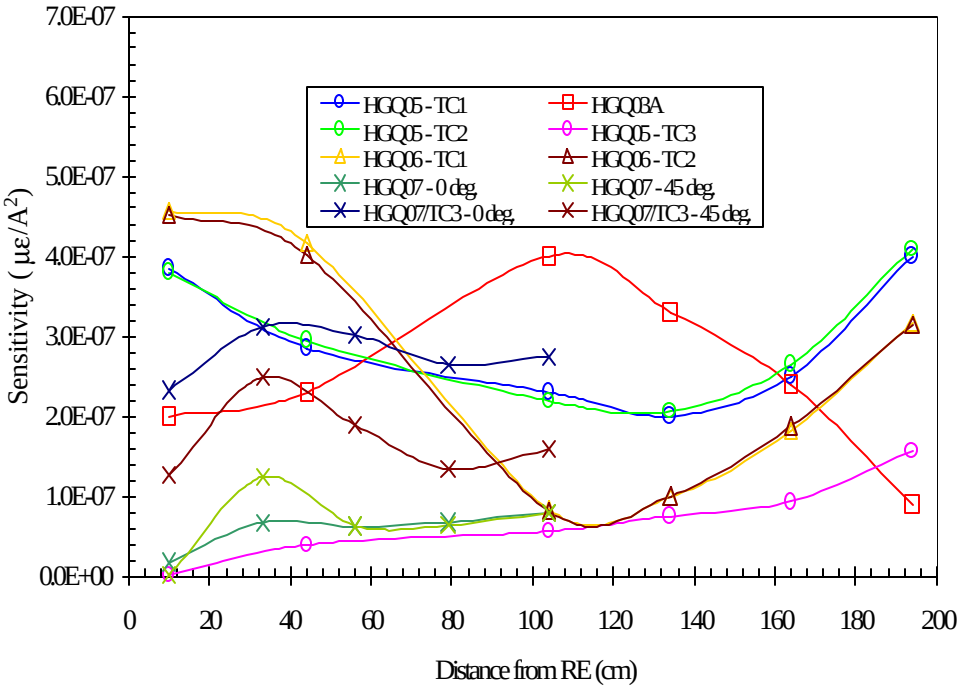

Figure 11. Longitudinal shell strain sensitivity along the cold mass length.

End loading was re-applied to the non-lead end of magnet HGQ07 for the third test cycle. This was accompanied by a return to non-zero strain at the non-lead end. Also, the distribution of strain along the cold mass length for magnet HGQ07 (and HGQ08 and HGQ09, as shown in Figure 12) is more uniform than for previous magnets.

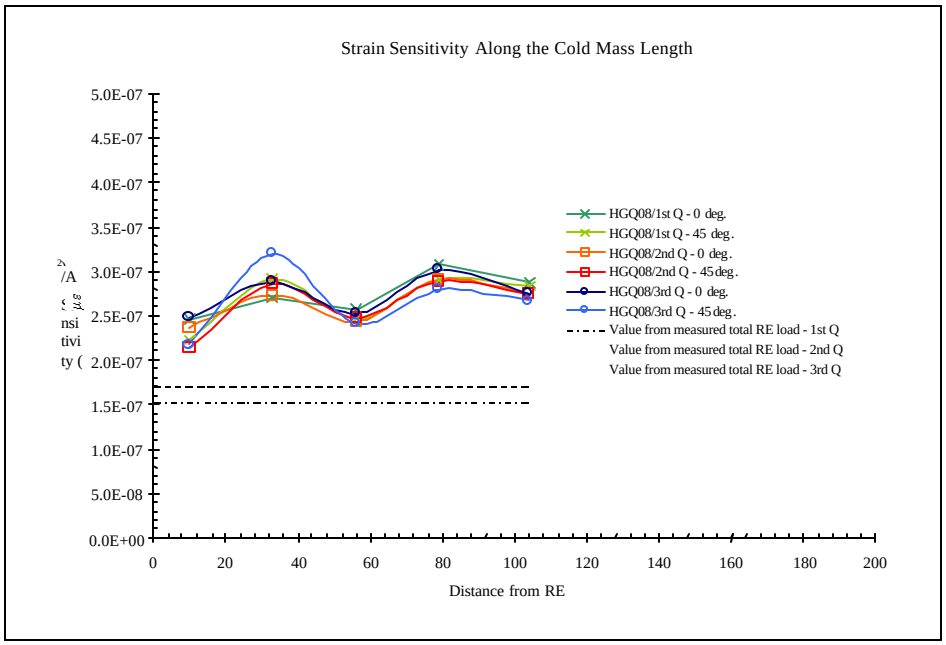

Figure 12. Strain sensitivity along the cold mass for magnet HGQ08, for several thermal cycles and two azimuthal positions. The dashed lines represent values expected from measured end forces.

4. Summary.

The Fermilab HGQ mechanical design appears to offer satisfactory coil support against mechanical disturbances in the body of the magnet. The mechanical design has been refined and improved through a combination of analytical, computational, and empirical studies. The essential design details leading to achievement of the performance goals have been finalized.

The range of coil prestresses that appear to provide adequate coil precompression and restraint is reasonably large (80±20 MPa), allowing for a coil size deviation in production of ±30 m, without any degradation to quench performance. Coil sizes and moduli, as described in Chapter 2, have been refined so that the minimal amount of shim is needed to reach the coil target size and prestress, while at the same time achieving a uniform distribution of prestress between the inner and outer coils.

While changes in end loading or restraint conditions had no observed effect on magnet quench performance, it was felt that longitudinal motion from thermal contraction should still be reduced, and positive longitudinal restraint maintained. This was accomplished by utilizing and aluminum end-can and G-11 collet structure to radially and longitudinally constrain the ends. This feature substantially reduced the longitudinal motion resulting from thermal contraction, and allowed positive contact to the end plates to be maintained with much lower initial room temperature end loads. While there is no empirical evidence that it has a positive effect on magnet performance, the design feature whereby the end cans are bolted to the end plates to prevent their longitudinal motion towards the center of the cold mass has been retained for the prototype design.

Since only ~ 25% of the calculated longitudinal Lorentz forces has been measured by the bullet gauges during operation at the design gradient, the end plate thickness has been

reduced from 50 mm to 35 mm. This is sufficient to adequately support the measured coil longitudinal loads and reduces the cold mass overall length.

REFERENCES

[1] US-LHC Technical Design Handbook, Chapter II.1.2.2

[2] M.J. Lamm et al., "A new facility to test superconducting accelerator magnets", PAC '97, Vancouver, Canada, 1997

[3] C.L. Goodzeit, M.D. Anerella, and G.L. Ganetis, "Measurement of Internal forces in superconducting accelerator magnets with strain gauge transducers", IEEE Trans. on Magnetics, vol. 25, no. 2, March 1989

[4] N. Siegel, D. Tommasinin, I. Vanenkov, "Design and use of capacitive force transducers for superconducting magnet models for the LHC", Proceedings of MT-15, Beijing, China, October 1997

[5] Fermilab Drawing FNAL 0102-MB-217987

[6] Measurements Group, Micro-Measurements Division, Raleigh, NC 27611, USA

[7] Fermilab Technical Note # TD-96-017

[8] J. P. Ozelis, "Development and Application of Capacitance Strain Gauges at Fermilab", presented at 1st International Capacitance Strain Gauge Workshop, LBNL, October 1998

[9] S. Yadav, J. Kerby, J.P. Ozelis, "Analysis of parameters affecting beam gauge performance", submitted to MT16, 1999.